

# DEPOSITION OF $\text{Nb}_3\text{Sn}$ FILMS BY MULTILAYER SEQUENTIAL SPUTTERING FOR SRF CAVITY APPLICATION\*

N. Sayeed<sup>†</sup>, H. E. Elsayed-Ali, Old Dominion University, Norfolk, Virginia, USA,

U. Pudasaini, The College of William and Mary, Williamsburg, Virginia, USA,

G. V. Eremeev, C. E. Reece, M. Burton, A.M. Valente-Feliciano, Thomas Jefferson National Accelerator Facility, Newport News, Virginia, USA

## Abstract

$\text{Nb}_3\text{Sn}$  is considered as an alternative of Nb for SRF accelerator cavity application due to its potential to obtain higher quality factors and higher accelerating gradients at a higher operating temperature. Magnetron sputtering is one of the effective techniques that can be used to fabricate  $\text{Nb}_3\text{Sn}$  on SRF cavity surface. We report on the surface properties of  $\text{Nb}_3\text{Sn}$  films fabricated by sputtering multiple layers of Nb and Sn on sapphire and niobium substrates followed by annealing at 950°C for 3 h. The crystal structure, film microstructure, composition and surface roughness were characterized by X-ray diffraction (XRD), scanning electron microscopy (SEM), energy dispersive X-ray spectroscopy (EDS), and atomic force microscopy (AFM). The RF performance of the  $\text{Nb}_3\text{Sn}$  coated Nb substrates were measured by a surface impedance characterization system. We also report on the design of a multilayer sputter deposition system to coat a single-cell SRF cavity.

## INTRODUCTION

Modern particle accelerators use Nb superconducting radiofrequency (SRF) cavities which are operated at 2 K to accelerate charged particles [1]. Significant improvement on the performance of Nb cavities have been made over last few decades and Nb cavities have reached close to theoretical limits. New alternative materials with high superconducting properties drew attention to replace Nb cavities.  $\text{Nb}_3\text{Sn}$  is considered as a promising alternative due to its high critical temperature  $T_c$  (18.3K) and high superheating field  $H_{sh}$  (400 mT) [2]. However, due to the fragile nature of the material, it is not used to fabricate cavities, but thin layer of superconducting  $\text{Nb}_3\text{Sn}$  film inside the surface of Nb or Cu cavities can enable the cavity to achieve higher quality factor with higher accelerating gradient even at higher operating temperature of 4.2 K. Sn diffusion technique used by Siemens in 1970's [3] is widely used technique to coat  $\text{Nb}_3\text{Sn}$  inside the cavity [4-6]. Another promising alternative is magnetron sputtering by which  $\text{Nb}_3\text{Sn}$  films have been successfully grown on small substrates [7-9]. According to the authors' knowledge, the method is successfully implemented for Nb coating inside Cu cavities [10-12] but have not been implemented to coat  $\text{Nb}_3\text{Sn}$  inside the cavity surface.

We have successfully deposited  $\text{Nb}_3\text{Sn}$  films on sapphire and Nb substrates by multilayer sputtering of Nb and Sn. The films were characterized by X-ray diffraction (XRD), scanning electron microscopy (SEM), atomic force microscopy (AFM), energy dispersive X-ray spectroscopy (EDS). The superconducting  $T_c$ , transition width  $\Delta T_c$  and residual resistivity ratio  $RRR$  were measured by four-point probe measurement system down to cryogenic temperature. RF surface resistance of  $\text{Nb}_3\text{Sn}$  films on Nb substrates were measured using the surface impedance characterization (SIC) system at Jefferson Lab [13]. Here, we report our recent progress on  $\text{Nb}_3\text{Sn}$  coating by multilayer sputtering. Besides, the primary design of a multilayer sputtering system to fabricate  $\text{Nb}_3\text{Sn}$  inside a single cell cavity has been reported.

## EXPERIMENTS

The experiment was carried out in two-step process: first, multilayers of Nb and Sn were deposited on substrates by a magnetron sputter coater, second the films were annealed at 950 °C for 3 hours for interdiffusion of Sn and Nb to form  $\text{Nb}_3\text{Sn}$ . AJA ATC Orion 5 Magnetron sputter coater was used to deposit Nb and Sn multilayers. The films were deposited on rotating substrate at 1 Å/s deposition rate. We have deposited three sets of films with different Nb buffer layer thickness. One set was deposited without any Nb buffer layer. Other two sets were coated with 20, and 100 nm buffer layer. 10 nm thick Sn layer and 20 nm thick Nb layer were deposited after depositing the buffer layer. The Sn and Nb layers were continued for 50 cycles to deposit 1.5 μm thick multilayers. The final layer was Nb to block Sn evaporation during annealing. All films were annealed at 950 °C for 3 h in a vacuum furnace. The coating description of the films is shown in Table 1.

The crystal structures of the films were analyzed by X-ray diffraction peaks obtained from Rigaku Miniflex II X-ray diffractometer using Cu-K $\alpha$  radiation. The surface morphology was investigated by Hitachi S-4700 Field Emission Scanning Electron Microscope. Film stoichiometry was estimated from data obtained from a Noran 6 energy dispersive X-ray spectroscopy (EDS) detector connected to a Jeol JSM 6060 LV scanning electron microscope using 15kV accelerating voltage. Surface roughness was measured by Digital Instrument Dimension 3100 Atomic Force Microscope (AFM) in tapping mode. Superconducting properties of the coated films were measured by four-point probe method in an isothermal measurement

\*Authored by Jefferson Science Associates, LLC under U.S. DOE Contract No. DE-AC05-06OR23177. The U.S. Government retains a non-exclusive, paid-up, irrevocable, world-wide license to publish or reproduce this manuscript for U.S. Government purposes.

<sup>†</sup>msaye004@odu.edu

system at varied temperature [14]. Based on the superconducting results, a Nb disk with 2" diameter was coated to measure the RF surface resistivity using the Surface Impedance Characterization system [13] at Jefferson Lab.

Table 1: The Coating Description of Deposited Films

	Sample Name	Buffer Layer Thickness (nm)	Nb Layer Thickness (nm)	Sn Layer Thickness (nm)	Total thickness (nm)
Sapphire substrate	T192	0	20	10	1500
	T188	20	20	10	1520
	T184	100	20	10	1600
Niobium substrate	M11	0	20	10	1500
	M0	20	20	10	1520
	M1	100	20	10	1600

## RESULTS AND DISCUSSIONS

### Structure and Morphology

The X-ray diffraction patterns of films on both sapphire and Nb substrate after annealing are shown in Figure 1. Both films were coated using 100 nm Nb buffer layer on the substrates. Films on both substrates showed different diffraction orders of  $\text{Nb}_3\text{Sn}$  phase. However, films on sapphire substrate showed few diffractions due to other phases of Nb and Sn (inset image). Diffraction peak of  $\text{Nb}_3\text{Sn}$  (211) couldn't be identified from the diffraction pattern of films on sapphire substrates due to strong diffraction peak from substrate at  $41.72^\circ$ .

Figure 2 shows SEM and AFM images of films coated on sapphire substrates without buffer layer and with 100 nm thick Nb buffer layer. As seen from the SEM images, the film without buffer layer has a surface with randomly distributed particles on top of grains. Comparison of EDS spectra on the region with particles with the region without particles revealed Sn reach value on these particles. These particles, however, did not affect the roughness of the films. The measured RMS roughness of the films were 33.71 and 34.65 nm for 0 and 100 nm buffer layers respectively. SEM micrograph of film on Nb substrate (0 nm buffer layer) is shown in Figure 3(a). For Nb substrate, all films showed surface with uniformly distributed grains of 100 nm to 400 nm with some voids. Films with all three conditions showed absence of Sn rich particles. During annealing process, two phenomena take place: diffusion of Sn into Nb, and evaporation of Sn from surface. These two phenomena depend on the annealing parameters (temperature, time, annealing rate etc.). On sapphire substrates, Sn near the substrate (1st layer) couldn't diffuse into the substrate and diffused into nearest Nb (1st layer), whereas on the Nb substrates or sapphire substrates with Nb buffer, Sn can diffuse into the substrate or into the buffer layer. As a result, Sn concentration near the surface was higher for the sapphire substrate without a buffer layer. These higher Sn concentrations experienced evaporation and escaped the top Nb layer and Sn rich particles were

formed by condensation during the cooldown process. These Sn rich particles were not found on films with thick Nb buffer layer on sapphire substrates and all films on Nb substrates because Sn diffused into the buffer layer and Nb substrates, resulting in less Sn near the surface for evaporation.

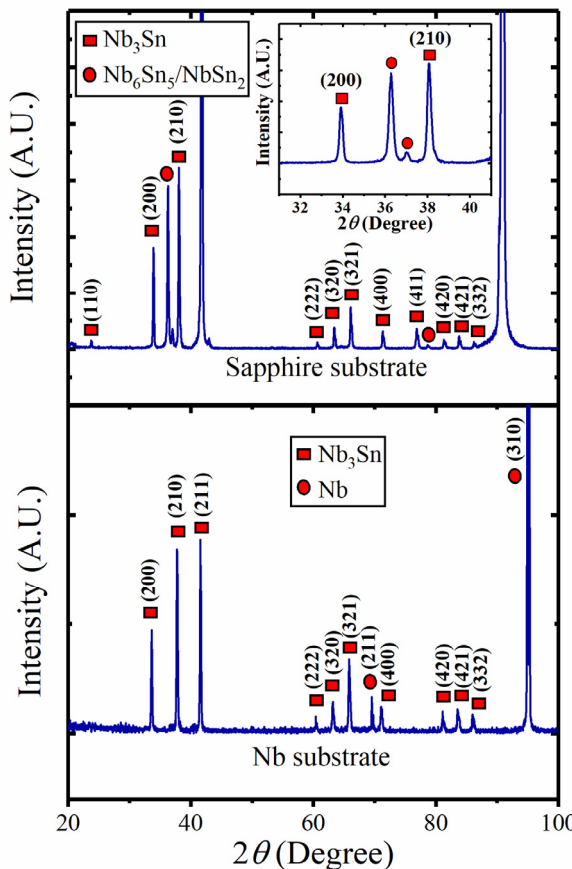


Figure 1: X-ray diffraction patterns of  $\text{Nb}_3\text{Sn}$  coated films on sapphire and Nb substrate.

Figure 3(b) and 3(c) show the AFM images ( $5 \mu\text{m} \times 5 \mu\text{m}$  scan area) of films with 0 nm and 100 nm buffer layer respectively on Nb substrate. Like the films on sapphire substrates, surface roughness of the films did

not vary significantly. The measured RMS roughness were 23.5 and 24.3 nm for films with buffer layers of 0 and 100 nm respectively. The atomic concentration observed in EDS are shown in Table 2. All annealed films experienced Sn loss due to evaporation.

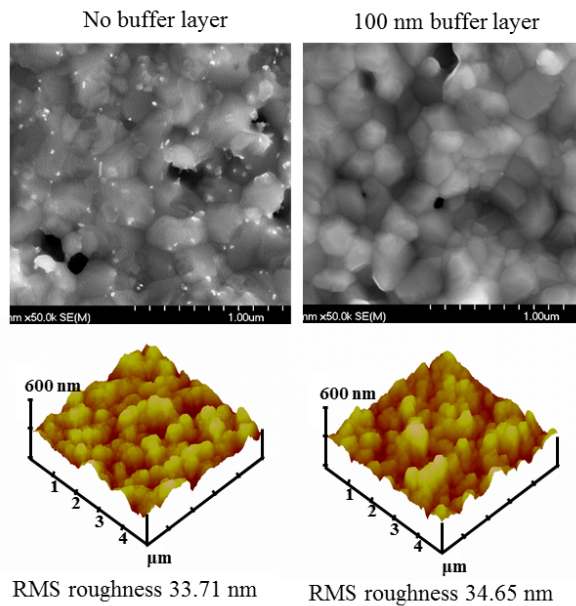


Figure 2: SEM and AFM images of  $\text{Nb}_3\text{Sn}$  coated films on sapphire substrate.

Table 2: EDS Data Showing Sn Concentration of the As-deposited and Annealed Samples

Sample Name	At. % of Sn As-deposited	At. % of Sn Annealed
T192	27	22
T188	27	22
T184	27	23
M11	27	22
M0	27	23
M1	27	22

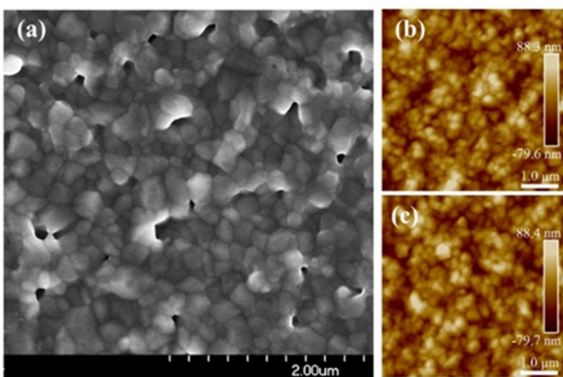


Figure 3: SEM and AFM images of  $\text{Nb}_3\text{Sn}$  coated films on Nb substrate: (a) SEM image of film with 0 nm buffer layer, (b) AFM image of film with 0 nm buffer layer, (c) AFM image with 100 nm buffer layer.

### $T_c$ Measurement

Figure 4 shows the resistance curve as a function of temperature measured by four-point probe method using a drive current of 10 mA. The corresponding critical temperature ( $T_c$ ), transition width ( $\Delta T_c$ ), and residual resistivity ratio ( $RRR$ ) are shown in Table 3. Films with all conditions showed superconducting  $\text{Nb}_3\text{Sn}$  with critical temperature ranging 17.75 – 17.82 K with narrow transition width.

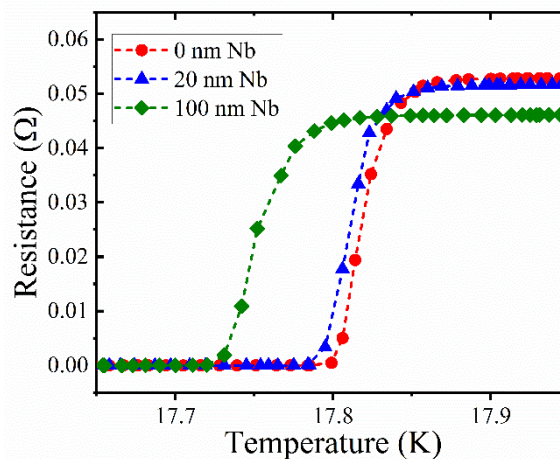


Figure 4: Resistance vs temperature curve of films with buffer layer of different thicknesses.

Table 3: Measured  $T_c$ ,  $\Delta T_c$ , and  $RRR$  of Films on Sapphire Substrates

Sample Name	$T_c$ (K)	$\Delta T_c$ (K)	$RRR$
T192	17.82	0.03	4.66
T188	17.81	0.03	4.69
T184	17.75	0.04	4.32

### RF Measurement

We coated Nb disk of 2" diameter using multilayer sputtering to measure the RF surface resistance. The 1.5  $\mu\text{m}$  thick film had 200 nm buffer layer and multilayers of 20 nm thick Nb and 10 nm thick Sn. The surface resistance of the film was compared with the previous SIC data of conventional vapor diffused  $\text{Nb}_3\text{Sn}$  sample [15]. Figure 5 shows the RF surface resistance as a function of temperature for both samples. Like vapor diffused samples, surface resistance of sputtered samples decreased sharply near 18 K. The sputtered sample showed another sharp drop on resistance near 8 K. This is due to the exposed Nb from the substrate which was covered by the sample holding clips during deposition (inset of Figure 5).

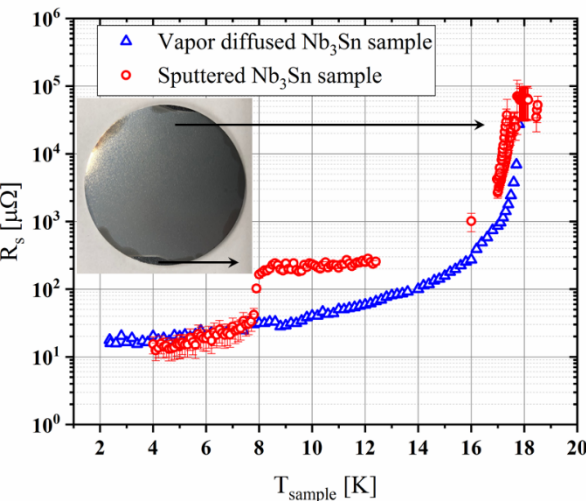


Figure 5: Surface resistance vs temperature curve of sputtered sample and vapor diffused sample.

## SPUTTER SYSTEM DESIGN

The goal of our current research is to establish a multilayer sputtering system to deposit Nb<sub>3</sub>Sn films inside a single-cell RF cavity. Both deposition and annealing should be performed without breaking the vacuum to minimize contamination. Therefore, we have designed a system that can be installed in current furnace used for vapor diffusion coating at Jefferson Lab. The design of the system is shown in Figure 6. Two sets of welded bellows will be used to control the movement of the sputter system. Bellow 1 will control the movement of magnets whereas bellow 2 will control the movement of the cathode. These two bellows will be moved simultaneously to coat the cavity surface. The whole cavity will be divided into three parts for coating: first, the top beam tube will be coated with multilayers, then the equator and bottom beam tube will be coated with similar coating cycles. Air will be used as cooling medium of the cathode during deposition. After deposition, the cathode will be raised up by expanding both bellows to thermally isolate the cathode from the furnace. Finally, the coated cavity will be annealed at desired temperature to fabricate Nb<sub>3</sub>Sn films.

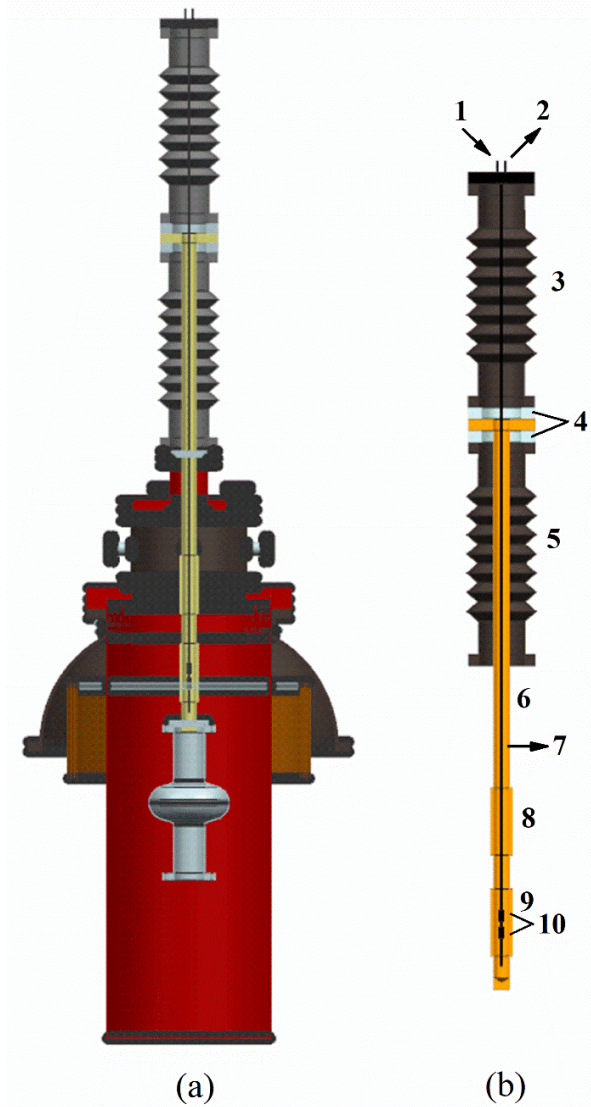


Figure 6: CAD design of the sputter system: (a) installed with the furnace, (b) different parts of the sputtering system: 1. cooling air inlet, 2. air outlet, 3. bellow 1, 4. ceramics to electrically isolate the cathode from the furnace, 5. bellow 2, 6. cathode tube, 7. magnet holder rod, 8. Sn target, 9. Nb target, and 10. magnets.

## CONCLUSION

We have successfully deposited Nb<sub>3</sub>Sn films on Nb and sapphire substrates by multilayer sequential sputtering method. The films experienced Sn deficiency after annealing due to evaporation from the surface. Films without buffer layer on sapphire substrate had randomly distributed Sn rich particles on top of the grains. The films on sapphire substrates have shown  $T_c$  up to 17.82 K. RF surface resistance of Nb<sub>3</sub>Sn film coated on Nb by multilayer sequential sputtering method was measured to be similar to surface resistance measured for the vapor diffused Nb<sub>3</sub>Sn films in SIC. Finally, preliminary design of a multilayer single cell RF cavity sputtering system is discussed.

## ACKNOWLEDGEMENTS

This material is based upon work supported by the U.S. Department of Energy, Office of Science, Office of Nuclear Physics. The authors acknowledge Michael J. Kelley, for his suggestions and Joshua Spradlin and James Henry for their support.

## REFERENCES

[1] H. Padamsee, J. Knobloch, and T. Hays, RF superconductivity for accelerators. Wiley Online Library, 2008.

[2] U. Pudasaini, G. Eremeev, C. E. Reece, J. Tuggle, and M. Kelley, "Initial growth of tin on niobium for vapor diffusion coating of Nb<sub>3</sub>Sn," *Superconductor Science and Technology*, 2018, doi: <https://doi.org/10.1088/1361-6668/aaafa88>.

[3] B. Hillenbrand, H. Martens, H. Pfister, K. Schnitzke, and G. Ziegler, "Superconducting Nb<sub>3</sub>Sn-cavities," *IEEE Transactions on Magnetics*, vol. 11, no. 2, pp. 420-422, 1975.

[4] S. Posen *et al.*, "Development of Nb<sub>3</sub>Sn Coatings for Superconducting RF Cavities at Fermilab", in Proc. 9th Int. Particle Accelerator Conf. (IPAC'18), Vancouver, Canada, Apr.-May 2018, pp. 2718-2720. doi:10.18429/JACoW-IPAC2018-WEPML016.

[5] R. D. Porter *et al.*, "Next Generation Nb<sub>3</sub>Sn SRF Cavities for Linear Accelerators", in Proc. 29th Linear Accelerator Conf. (LINAC'18), Beijing, China, Sep. 2018, pp. 462-465. doi:10.18429/JACoW-LINAC2018-TUP0055.

[6] U. Pudasaini *et al.*, "Nb<sub>3</sub>Sn Multicell Cavity Coating at JLab", in Proc. 9th Int. Particle Accelerator Conf. (IPAC'18), Vancouver, Canada, Apr.-May 2018, pp. 1798-1803. doi:10.18429/JACoW-IPAC2018-WEYGBF3.

[7] E. Ilyina *et al.*, "Development of sputtered Nb<sub>3</sub>Sn films on copper substrates for superconducting radiofrequency applications," *Superconductor Science and Technology*, vol. 32, no. 3, p. 035002, 2019, <https://doi.org/10.1088/1361-6668/aaaf61f>.

[8] L. Xiao *et al.*, "The Study of Deposition Method of Nb<sub>3</sub>Sn Film on Cu Substrate", in Proc. 18th Int. Conf. RF Superconductivity (SRF'17), Lanzhou, China, Jul. 2017, pp. 131-133. doi:10.18429/JACoW-SRF2017-MOPB036.

[9] M. N. Sayeed, U. Pudasaini, C. E. Reece, G. Eremeev, and H. E. Elsayed-Ali, "Structural and superconducting properties of Nb<sub>3</sub>Sn films grown by multilayer sequential magnetron sputtering," *Journal of Alloys and Compounds*, vol. 800, pp. 272-278, <https://doi.org/10.1016/j.jallcom.2019.06.017>.

[10] S. Calatroni, "20 Years of experience with the Nb/Cu technology for superconducting cavities and perspectives for future developments," *Physica C: Superconductivity*, vol. 441, no. 1-2, pp. 95-101, <https://doi.org/10.1016/j.physc.2006.03.044>.

[11] E. Chiaveri and W. Weingarten, "Industrial production of superconducting niobium sputter coated copper cavities for LEP," *SRF93*, p. 746, 1993.

[12] M. C. Burton, A. D. Palczewski, H. L. Phillips, C. E. Reece, A-M. Valente-Feliciano, and R. A. Lukaszew, "RF Results of Nb Coated SRF Accelerator Cavities via HiPIMS", in *Proc. 29th Linear Accelerator Conf. (LINAC'18)*, Beijing, China, Sep. 2018, pp. 427-430. doi:10.18429/JACoW-LINAC2018-TUP0042.

[13] B. P. Xiao, C.E. Reece, H.L. Phillips, R. L. Geng, H. Wang, F. Marhauser, M.J. Kelley, "Note: Radio frequency surface impedance characterization system for superconducting samples at 7.5 GHz", *Rev. Sci. Inst.*, 82 (5) 056104, (2011) doi:10.1063/1.3575589.

[14] J. K. Spradlin, C. E. Reece, and A-M. Valente-Feliciano, "A Multi-Sample Residual Resistivity Ratio System for High Quality Superconductor Measurements", in *Proc. 17th Int. Conf. RF Superconductivity (SRF'15)*, Whistler, Canada, Sep. 2015, paper TUPB063, pp. 726-730.

[15] G. V. Eremeev, H. L. Phillips, A-M. Valente-Feliciano, C. E. Reece, and B. P. Xiao, "Characterization of Superconducting Samples With SIC System for Thin Film Developments: Status and Recent Results.", in *Proc. 16th Int. Conf. RF Superconductivity (SRF'13)*, Paris, France, Sep. 2013, paper TUP070, pp. 599-602.